Methodology for Reliability Analysis of Reinforced Concrete Structures over time Considering Combined Corrosion

Ana Carolina Cavalcanti Moraes[1], Renato de Siqueira Motta[1], Silvana Maria Bastos Afonso da Silva[1], Eleni Toumpanaki[2], Raffaele De Risi[2].

[1] *Dept. of Civil Engineering, Federal University of Pernambuco*
Av. Prof. Moraes Rego, 1235 - Cidade Universitária, Pernambuco/Recife, Brazil
ana.accm@ufpe.br, renato.motta@ufpe.br, silvana.bastos@ufpe.br
[2] *Dept. of Civil Engineering, University of Bristol*
Queen's Building University Walk, BS8 1TR, Bristol, UK
eleni.toumpanaki@bristol.ac.uk, raffaele.derisi@bristol.ac.uk

Abstract. One of the main causes of deterioration in reinforced concrete structures (RC) is the corrosion of steel rebars. Many factors, including materials, environments, and loading conditions, which often have uncertain characteristics, affect the performance of RC structures. Some uncertainties may depend on time and location, and associated reliability issues become more difficult to address. This study presents a comprehensive method for assessing the temporal reliability of reinforced concrete structures, taking into account the combined effects of carbonation and chloride penetration. Probabilistic models are used to capture uncertainties related to the beginning, propagation, and combined effects of corrosion on structural performance over time. The time-dependent reliability of bridge structures is evaluated using sophisticated numerical simulations in conjunction with the Monte Carlo method for reliability analysis. Through the methodology presented here, engineers and decision-makers can assess the reliability of reinforced concrete structures using a systematic framework that considers the complex interactions of corrosion mechanisms. This aids maintenance planning and effective resource allocation to ensure long-term structural safety and durability. Considering a case from the literature as a source, the reliability analysis with combined effects was tested on a reinforced concrete bridge beam with corroded steel reinforcing bars. The results show that the model is acceptable for assessing structural reliability along the RC structure life cycle.

Keywords: Combined Corrosion Model, Reliability Analysis, Reinforced Concrete Structures.

1 Introduction

According to Abd Elmoaty [1], a variety of aggressive agents and environmental conditions can affect reinforced concrete structures during their service life, such as exposure to sulphates, chlorides and seawater, and wetting and drying, and freezing and thawing conditions. The most significant deterioration process that affects the safety of concrete structures is the corrosion of reinforced steel . Di Sarno and Pugliese [2] consider that steel rebar volume increases as a consequence of carbonation and chloride penetration, which also result in the formation of corrosion products like rust. The main effects are strain tensile strain concentrations between the concrete and the steel reinforcements and consequently micro-cracks inside the concrete. These can lead to reinforced concrete deterioration, including concrete cover spalling, decrease in concrete compressive strength, lack of concrete confinement from transverse reinforcement, buckling and loss of tensile area of reinforced bars

Recent studies (e.g., Pugliese, De Risi and Di Sarno [3]; Di Sarno and Pugliese [4]) showed that, worldwide, a large number of reinforced concrete (RC) structures, particularly bridges, are currently suffering from deterioration as a result of exposure to harsh environmental factors and rising live loading as a result of sharp increase in traffic volume. Bridges' anticipated service life is frequently shortened by inadequate or non-existent maintenance, which may result in structural collapse in severe circumstances. Although corrosion is unpredictable

and complex, making it difficult to model and simulate, it is necessary to assess the remaining capacity of old RC infrastructure using advanced structural reliability methodologies.

Frangopol et al. [5] show that comparing the accepted and actual probability of failure (P_f) is important, and in this context, structural reliability methods provide an effective means of evaluating the state of infrastructure over its life cycle, accounting for all pertinent uncertainties. This paper presents an application of a structural temporal reliability analysis in a representative beam from a RC bridge with corroded steel reinforcement bars originally described in Li et al. [6], simplifying a real case scenario. In this case, a combination of numerical models and code-based techniques are used to calculate the bridge girder's capacity. Specifically, the methodology proposed by Li J et al. [6] takes into account both general and pitting corrosion, as well as their combination to produce a more sophisticated study. To quantify the reduction of longitudinal and transversal reinforcement rebar area owing to corrosion, a straightforward method is utilized to account for degradation occurrences.

In this study, the corrosion model for steel reinforcing bars is the only ageing mechanism taken into account. This study serves as the basis for future work, which will include the general, pitting, and compound corrosion models into an existing bridge reliability analysis while also accounting such as additional random variables. The uncertainty is propagated and the distributions of the capacity and demand for the girder beam in terms of bending moment are calculated using a Monte Carlo simulation.

2 Corrosion Models

Considering Revert et al. [7] a reinforced concrete structure's design service life can be determined by a limit state and the degree of reliability for failing it. Reinforced concrete structures usually have two service lives: an initiation period and a propagation period. The amount of time that harmful elements can permeate the cover and continue to cause active corrosion is known as the initiation period. Damage grows during the propagation phase until it reaches an intolerable state of decline. Depassivation of the steel reinforcement is the limit condition commonly employed for service life design in carbonating reinforced concrete constructions. However, following Angst et al. [8], there are other requirements for active corrosion besides carbonation of the steel-concrete interface. There is a chance that the propagation time will alternate between active and passive corrosion depending on the moisture content.

Based on Dai, L. [9] steel corrosion caused by chloride is one of the main causes of degradation in concrete buildings. In recent times, certain prestressed concrete (PC) constructions that are already in place have also been shown to exhibit strand corrosion-related deterioration. High-stress strands are more likely to corrode than regular steel. Experience in the field and findings from experiments indicate that structures impacted by corrosion lose their serviceability faster than their safety. According to Stewart and Al-Harthy [10] when reinforcing steel bars are exposed to corrosion caused by chloride, pitting corrosion frequently occurs. This could result in a large-scale, highly localized loss of section, which would be extremely dangerous for the structural integrity.

In addition to corrosion caused by chloride, Wang, Yue & Qiang [11], Li et al. [12], and De Weerdt et al. [13] says that carbonation-induced corrosion is a major factor that deteriorates reinforced concrete structures throughout their service life in a variety of climatic circumstances. The interaction between airborne carbon dioxide (CO_2) and the calcium hydroxide ($Ca(OH)_2$) in concrete is generally responsible for the carbonation of PC concrete, causing the pore solution's alkalinity to drop. The Pourbaix diagram shows that when iron or steel is exposed to a low-alkalinity environment, the oxide deposit on the material becomes unstable. Because of this instability, faulty iron hydroxide is formed, which leads to the development of steel corrosion.

This model proposed by Li et al. [6] develops a coupled corrosion model shown in Fig.1. This model combines the impacts of pitting and general corrosions representative of real-world engineering applications. One corrosion mechanism may predominate over another in different situations. For instance, general corrosion is the predominant corrosion mechanism in atmospheric media. However, the most common type of corrosion in a marine environment is pitting corrosion. All of the equations applied in this application are presented in Li et al. [6].

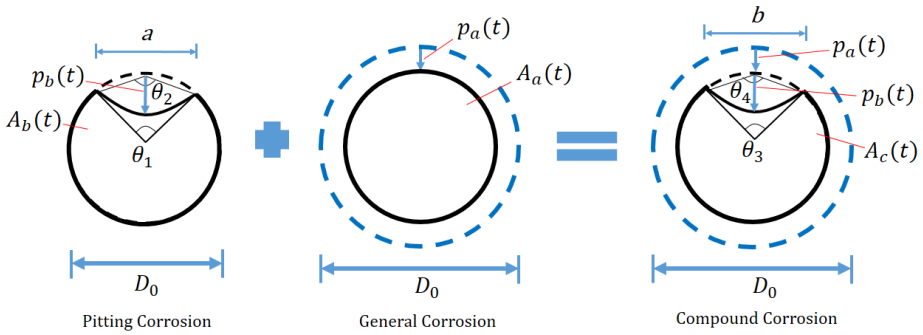

Figure 1. Compound corrosion of a steel bar scheme adapted from Li et al. [6]

3 Case Study

Following the study conducted by Li et al. [6], this section examines the temporal reliability analysis of a RC bridge with corroded steel reinforcement bars. Fig. 2 shows a simplified schematic diagram of the girder of the bridge, which consists of a single beam and two columns. A focused force F(t) (N) at the midpoint of the beam, and a uniformly distributed load, w (N/m), are applied to the beam.

The load temporal variability is caused by the force $F(t)$, which varies randomly over time, represented by a stochastic process. The concrete cover depth, c(x), is considered to vary spatially along the concrete surface in this example. The area of the bars varies with time following the corrosion model. This will cause the spatial variation of the corrosion and propagation time, and, consequently, the spatial variation of the corroded areas. The temporal and spatial variability are represented by the stochastic process and random field, respectively.

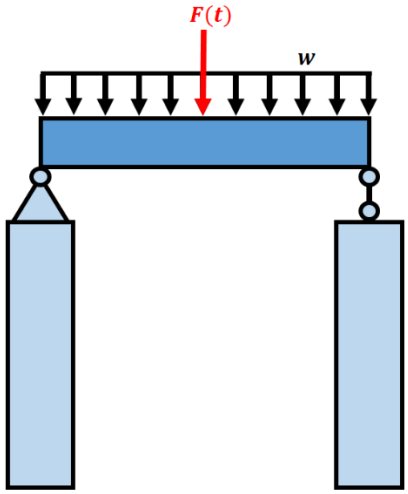

Figure 2. Diagram of the bridge adapted from Li et al. [6]

The beam under consideration has a rectangular cross-section with width b (m) and height h (m). The beam has a length L (m), and there are n_b = 4 steel bars inside the concrete. Fig. 3 displays the bending moment diagram and cross-section diagram. The equations adopted for the study and analysis are presented in Li et al. [6].

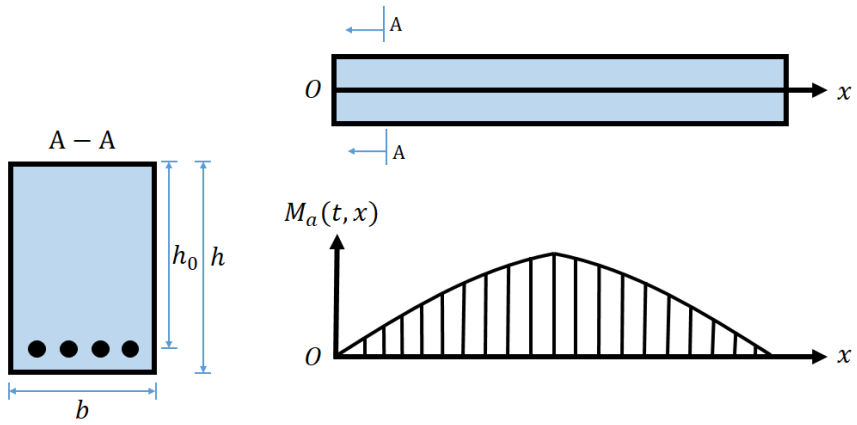

Figure 3. Bending moment diagram and cross-section adapted from Li et al. [6]

4 Reliability Analysis

According to Song & Kawai [14], analytical or numerical integration can be used to approximate the chance of failure, however, analytical integration is limited to exceptional and uncommon circumstances that are frequently of little or no practical use. Because the convergence rate of Monte Carlo Simulation (MCS) is insensitive to the dimensionality of the input variable and the limit state function, it has been frequently used in structural reliability analysis. MCS attempts to sample the input variable and repeatedly evaluate the limit state function directly, as opposed to estimating or surrogating the function. The reliability analysis has been conducted via the MCS simulation method, considering the random variables shown in Table 1, and executed on Matlab. The simulation was made until T = 100y (year by year), and $N = 10^5$. The failure function can be written as Eq.1.

$$G(\boldsymbol{X}, \boldsymbol{Y}(t), \boldsymbol{Z}(x), t, x) = M_u(t,x) - M_a(t,x) = f_y A_u(t,x)\left[h_0(x) - \frac{f_y A_u(t,x)}{2 f_c b}\right] - M_a(t,x). \quad (1)$$

Where t represents the time variable varying within [0, T]; x is the space variable varying in [0, L]; X=[ka, D_0, C_b, D_b, C_{cr}, lb, b, h, fy, fc, w] are random variables; Y(t)= [F(t)] is a Gaussian stochastic process; Z(x)=[c (x)] is a Gaussian random field; $h_0(x)$ is the effective height; $Mu(t,x)$ is the bending moment capacity; $Au(t,x)$ is the remaining cross-sectional area of a corroded steel bar and $Ma(t,x)$ is the bending moment of RC beam.

The bending moment capacity of the RC beam is detailed in Eq.2.

$$M_u(t,x) = f_y A_u(t,x)\left[h_0(x) - \frac{f_y A_u(t,x)}{2 f_c b}\right]. \quad (2)$$

The remaining cross-sectional area of reinforcing steel at time t (considering corrosion of the $n_b$bars) is shown in Eq.3.

$$A_u(t,x) = n_b A_c(t,x). \quad (3)$$

And the bending moment M_a of the RC beam is calculated as from Eq.4 or Eq.5.

$$M_a(t,x) = \frac{F(t)}{2}x + \left(\frac{wL}{2}x - \frac{wL}{2}x^2\right), 0 \le x \frac{L}{2}. \quad (4)$$

$$M_a(t,x) = \frac{F(t)}{2}(L-x) + \left(\frac{wL}{2}x - \frac{wL}{2}x^2\right), \frac{L}{2} < x \le L. \quad (5)$$

Table 1. Random variables considered for the reliability method by Li et al. [6]

Parameter	Distribution	Mean	Coefficient of variation
k_a (mm/year$^{0.5}$)	Normal	3	0.30
D_0 (mm)	Normal	ϕ18	0.05
C_b (kg/m^3)	Lognormal	3.5	0.20
D_b (m^2/s)	Lognormal	$12*10^{-12}$	0.20
C_{cr} (kg/m^3)	Uniform	0.9	0.20
λ_b	Gumbel	6	0.20
b (mm)	Normal	600	0.05
h (mm)	Normal	800	0.05
f_y (MPa)	Lognormal	400	0.10
fc (MPa)	Lognormal	30	0.15
w (N/m)	Normal	$4*10^4$	0.10
F(t) (N)	Gaussian process	10^5	0.20
c(x) (mm)	Gaussian field	30	0.20
W/C	Deterministic	0.4	-
T (years)	Deterministic	100	-
L (m)	Deterministic	5	-

k_a (mm/year$^{0.5}$) is the concrete carbonation coefficient; D_0 (mm) is the initial diameter of steel bar; C_b (kg/m^3) is the surface chloride concentration; D_b (m^2/s) is the chloride diffusion coefficient; C_{cr} (kg/m^3) is the chloride threshold level; λ_b is the ratio coefficient that varies from 4 to 8; b (mm) is the width of the beam; h (mm) is the height of the beam; f_y (MPa) is the steel yield stress; fc (MPa) is the concrete compressive strength; w (N/m) is a uniformly distributed load; c(x) (mm) is the concrete cover depth of steel; W/C is the water-cement ratio; L (m) is the length of the beam.

Fig. 4 shows three realizations (from $N = 10^5$) of the Gaussian random field, c(x), each representing variations in cover depth along half length of the RC beam under consideration (in millimeters) due to symmetry. This suggests areas with potentially different levels of protection against environmental factors. The smoothness and continuity of the trajectories show the correlation structure of the Gaussian random field, or how values are associated across distance. Smoother trajectories are produced by a more highly correlated field, whereas more jagged lines are produced by a less correlated field. The variations of the trajectories are visually in accordance with data from Li et al. [6].

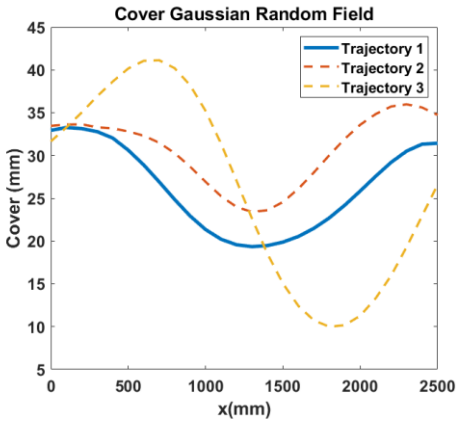

Figure 4. Trajectories of the Random Field.

Taking as example the cover depth in trajectory 1, Fig.5 shows the evolution of the failure function G(x,t) in a reliability analysis. Again, because of the symmetry, only half of the beam length is shown. There is a general downward trend in the failure function G(x,t) as x tends to the midpoint of the beam (2500 mm). This indicates that the structural capacity or safety margin tends to decrease along the middle of the structure. Initially (T = 0 years), most trajectories start with a positive value of G around 300 KNm at the column and 150KNm at the midpoint. As time progresses the G trajectories decrease due to corrosion. In locations with lower concrete cover (c) the corrosions starts earlier and the decrease in the G value is prominent. The figure highlights the importance of the cover variability to the failure of the beam, as the corrosion progresses.

The trajectories show a significant amount of variability over time, with some trajectories indicating a positive (G) (implying no failure) and others dipping into negative values (indicating failure). The point where G(x,t) crosses the zero line is critical. Trajectories crossing from positive to negative values indicate the transition from safe to failure states. The plot shows many such crossings, particularly after 1000 mm, suggesting potential locations where the structure might fail. This highlights the importance of considering variability and uncertainty in the reliability analysis. The failure function G(x,t) provides critical insights into the regions of the structure that are more likely to fail. The downward trend and multiple crossings of the zero line indicate several potential points of failure along the length of the structure. The high variability suggests that a probabilistic approach is essential for a reliable safety assessment. Deterministic methods may not capture the full extent of the risk.

In the reliability analysis, as depicted in Fig.5, the failure function decreases with the distance to the support and time, with a higher P_f in the midsection (x = 2500 mm) and for lower cover values. Critical regions have been identified where the likelihood of failure is significantly higher, providing valuable information for maintenance planning and design improvements. Quantifying the P_f at various points helps in making informed decisions to ensure the long-term safety and durability of reinforced concrete structures. For the realization shown in Fig.5, the failure occurred at t = 18y at the midspan. The x mark represents where this failure occurred (G = -7.1227).

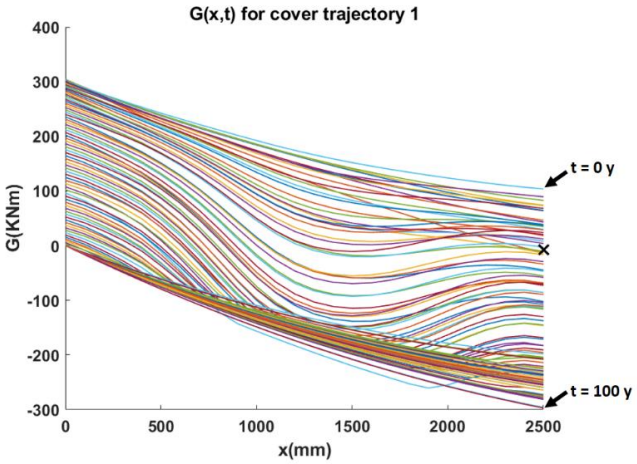

Figure 5. Failure Function G(x,t) - for cover trajectory 1.

Fig.6 shows the P_f of the RC beam over time, with the x-axis representing time in years and the y-axis representing the P_f. In the first 20 years, the probability of the beam's failure increases rapidly. This indicates that the beginning of the beam's lifespan shows a significant growth in the chance of failure, which is related to the reinforcement degradation. The initial structural assessment indicates a high P_f of 17%, where no corrosion has been activated, and increases as corrosion advances. The higher corrosion activity is, probabilistically, around 20y. After 40y the PF is almost 100%. After that time, failure becomes inevitable, and reinforcement or replacement measures would be necessary to ensure structural safety. Fig.6 shows a typical cumulative distribution function shape. The results shown in the literature have a similar P_f at the beginning of the analysis, but the degradation evolution contrasts with the present result.

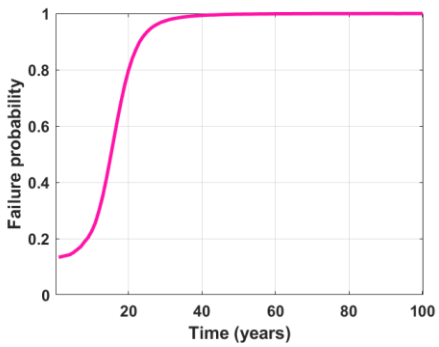

Figure 6. Probability of failure for the RC beam.

5 Conclusions

In this work, a corrosion model's application and reliability analysis were presented. The main focus has been on implementing a compound corrosion model in a simplified version of a realistic case of a bridge, which involves two types of simultaneous steel reinforcement corrosion. The key conclusion is that the compound corrosion model, which takes pitting and general corrosion into account, produces good results when constructed using the suggested model. As would be predicted, the failure function $G(x,t)$ has a decreasing trend when moving away from support ($x = 0$), and reaches its minimum value at the middle of the spam ($x = 2500$), considering the bending moment with notable variability. It is important to note that the obtained failure probability plot follows an acceptable pattern from the literature, but the result obtained by Li et al. [6] shows corrosion that seems to start immediately, presenting a rapid growth pattern of the failure probability right at the beginning.

The present work provides key contributions, providing a systematic framework for assessing the reliability of RC bridges considering complex corrosion interactions. It can be developed further as a tool for informed maintenance planning and resource allocation. The research offers valuable insights for engineers and decision-makers to evaluate the long-term safety and durability of RC structures. By understanding time-dependent reliability, effective maintenance strategies can be developed to prevent failures and extend the lifespan of these critical infrastructure components.

Acknowledgements. The authors would like to thank FACEPE (Fundação de Amparo à Ciência e Tecnologia do Estado de Pernambuco), FINEP, Coordenação de Aperfeiçoamento de Pessoal de Nível Superior (CAPES) and Conselho Nacional de Desenvolvimento Científico e Tecnológico (CNPq) for the financial support of various research projects developed in this area by the group.

Authorship statement. The authors hereby confirm that they are the sole liable persons responsible for the authorship of this work, and that all material that has been herein included as part of the present paper is either the property (and authorship) of the authors, or has the permission of the owners to be included here.

References

[1] M. Abd Elmoaty. Four-years carbonation and chloride induced steel corrosion of sulfate-contaminated aggregates concrete. *Construction and Building Materials*, v. 163, p. 539-556, 2018.
[2] L. Di Sarno, F. Pugliese. Numerical evaluation of the seismic performance of existing reinforced concrete buildings with corroded smooth rebars. *Bull Earthquake Eng*, v. 18, p. 4227–4273, 2020.
[3] F. Pugliese, R. De Risi & L. Di Sarno. Reliability assessment of existing RC bridges with spatially-variable pitting corrosion subjected to increasing traffic demand. *Reliability Engineering & System Safety*, v. 218, p. 108137, 2022.
[4] L. Di Sarno, & F. Pugliese. Effects of mainshock-aftershock sequences on fragility analysis of RC buildings with ageing. *Engineering Structures*, v. 232, 111837, 2021.
[5] D. M. Frangopol, J. S. Kong, and E. S. Gharaibeh. "Reliability-based life-cycle management of highway bridges". *Journal of computing in civil engineering*, v. 15(1), p. 27-34, 2021.
[6] J Li, J Chen, J Wei, X Yang. Temporal-spatial reliability analysis of RC bridges with corroded steel reinforcement bars. *Proceedings of the Institution of Mechanical Engineers, Part C: Journal of Mechanical Engineering Science*, v. 236, n.23, p.11345-11357, 2022.
[7] A. B. Revert, T. Danner, & M. R. Geiker. Carbonation and corrosion of steel in fly ash concrete, concluding investigation of five-year-old laboratory specimens and preliminary field data. *CEMENT*, v. 16, p. 100105, 2024.
[8] U. Angst, F. Moro, M. Geiker, S. Kessler, H. Beushausen, C. Andrade, & M. Serdar. Corrosion of steel in carbonated concrete: mechanisms, practical experience, and research priorities–a critical review by RILEM TC 281-CCC. *RILEM technical letters*, v. 5, p. 85-100, 2020.
[9] L. Dai, L. Wang, J. Zhang, & X. Zhang. A global model for corrosion-induced cracking in prestressed concrete structures. *Engineering Failure Analysis*, v. 62, p. 263-275, 2016.
[10] M. G. Stewart, & a. Al-Harthy. Pitting corrosion and structural reliability of corroding RC structures: Experimental data and probabilistic analysis. *Reliability engineering & system safety*, v. 93, n.3, p. 373-382, 2008.
[11] D. Wang, Y. Yue, & J. Qian. Effect of carbonation on the corrosion behavior of steel rebar embedded in magnesium phosphate cement. *Composites Part B: Engineering,v. 268,* p. 111088, 2024.
[12] Y. Li, T. Mi, W. Liu, Z. Dong, B. Dong, L. Tang, & F. Xing. Chemical and mineralogical characteristics of carbonated and uncarbonated cement pastes subjected to high temperatures. *Composites Part B: Engineering*, v. 216, p.108861, 2021.
[13] K. De Weerdt, G. Plusquellec, A. B. Revert, M. R. Geiker, & B. Lothenbach. Effect of carbonation on the pore solution of mortar. Cement and Concrete Research, v. 118, p.38-56, 2019.
[14] C. Song & R. Kawai. Monte Carlo and variance reduction methods for structural reliability analysis: A comprehensive review. *Probabilistic Engineering Mechanics*, v. 73, p. 103479, 2023.